

Evaluating natural language processing models with generalization metrics that do not need access to any training or testing data

Yaoqing Yang¹, Ryan Theisen¹, Liam Hodgkinson^{1,2}, Joseph E. Gonzalez¹,
Kannan Ramchandran¹, Charles H. Martin⁴, Michael W. Mahoney^{1,2,3}

¹ University of California, Berkeley

² International Computer Science Institute

³ Lawrence Berkeley National Laboratory

⁴ Calculation Consulting

Abstract

The search for effective and robust generalization metrics has been the focus of recent theoretical and empirical work. In this paper, we discuss the performance of natural language processing (NLP) models, and we evaluate various existing and novel generalization metrics. Compared to prior studies, we (i) focus on NLP instead of computer vision (CV), (ii) focus on generalization metrics that predict test error instead of the generalization gap, (iii) focus on generalization metrics that do not need the access to data, and (iv) focus on the heavy-tail (HT) phenomenon that has received comparatively less attention in the study of deep neural networks (NNs). We extend recent HT-based work which focuses on power law (PL) distributions, and we study exponential (EXP) and exponentially truncated power law (E-TPL) fitting to the empirical spectral densities (ESDs) of weight matrices. Our detailed empirical studies show that (i) *shape metrics*, or the metrics obtained from fitting the shape of the ESDs, perform uniformly better at predicting generalization performance than *scale metrics* commonly studied in the literature, as measured by the *average* rank correlations with the generalization performance for all of our experiments; (ii) among forty generalization metrics studied in our paper, the **rand.distance** metric, a new shape metric invented in this paper that measures the distance between empirical eigenvalues of weight matrices and those of randomly initialized weight matrices, achieves the highest worst-case rank correlation with generalization performance under a variety of training settings; and (iii) among the three HT distributions considered in our paper, the E-TPL fitting of ESDs performs the most robustly.

1 Introduction

Recent years have seen rising interest in large-scale empirical studies of the various metrics used to quantify generalization [1–4]. On the one hand, theory-driven metrics have the potential to reveal more information than test error and thus bring us one step closer to unpacking the black box of deep NNs [5–7]. On the other hand, a wide variety of generalization metrics have been applied to predict the *quality* of pretrained models [3, 8], design effective training procedures [9, 10], improve network efficiency [11, 12], quantify network robustness [13, 14], improve ensemble learning techniques [15, 16], analyze and improve large-scale contests [4], and so on.

Despite advances in the study of generalization, however, several recent papers point out the deficiencies of many of these “fantastic” generalization metrics. These include a lack of “robustness” to the changes of environmental hyperparameters [1, 2] (such as data, network architecture and training schemes), or the Simpson’s paradox that generalization metrics perform differently (i.e., predict opposite trends) when applied to each sub-part of a collection of learning models or to the holistic study [4]. Another drawback is the over-reliance on experiments with CV models, which are relatively well-explored, and which are not representative of many other application areas. Despite a few counterexamples [3, 5, 17], systematic studies of generalization in other fields, such as NLP, are largely missing.

Generalization metrics for NLP. The objective of this paper is to provide a systematic study of generalization metrics to address issues that have not received proper attention in prior studies [1–3]. We will primarily focus on NLP. Compared to CV, predicting generalization in NLP has several important differences that require careful consideration. The first is that training NLP models to completely interpolate the training data is often impossible, due to the web-scale size of the training data. This creates an issue when applying most existing generalization metrics because most of them focus on predicting the *generalization gap* (i.e., the difference between training and test performance) rather than the test error itself.

To see why focusing on the generalization gap is an issue, consider the most commonly used application to motivate the study of generalization metrics: comparing two models [4, 18].¹ Suppose two classification models A and B have 5% and 10% training error, respectively. In this case, even if a generalization metric correctly predicts that the model B has a smaller generalization gap than model A, and even if we know the training errors of both model A and B, it is still unclear if model B indeed has a smaller test error than A. In this paper, we aim to study generalization metrics that correlate with *model quality*, and we use test error as a close approximation of model quality. On the other hand, as we will demonstrate, (rank) correlation with the generalization gap does not imply (rank) correlation with model quality, as many of generalization metrics we study are on a substantially different scale from the values of the test error. Metrics that focus on predicting the generalization gap include most of the well-known metrics in CV, such as those based on the PAC-Bayesian framework [19, 20] and margins [21–23]. Therefore, from a practical point of view, for NLP tasks, we prefer generalization metrics that can directly predict the trends in test error (or similar evaluation metrics in NLP, such as the test BLEU score [24]) rather than trends in the generalization gap, so that we learn information closer to the model quality. Although this paper focuses on data-independent metrics, we also provide results for data-dependent metrics motivated by margins and PAC-Bayesian bounds [1, 2]. However, although these metrics perform well in predicting the generalization gap, we show that none of them satisfactorily predicts test error directly.

The second difference between NLP models and CV is that the data for NLP pretraining are usually web-scale and are hard to access and use, while the training data from standard CV benchmarks can often be easily obtained. Therefore, it will be ideal if the generalization metric under study could measure the quality of learning models *without access to data*. In this paper, we focus on generalization metrics that do not need access to data. Although surprising, recent work has shown that access to training or testing data is not necessary for assessing the model quality of learning models [3].

With these objectives in mind, among the generalization metrics in the literature, we take particular interest in those derived from the heavy-tail self regularization (HT-SR) theory [8, 25], which (i) predicts test error directly instead of the generalization gap and (ii) does not require access to training (or testing) data. In addition to these two advantages, there are several other benefits worth mentioning. First, it is known that NLP training is harder than benchmark image classification tasks and its optimization loss landscape can be problematic [17]. Therefore, the focus of the evaluation of NLP models should place more emphasis on the quality of the entire training process instead of the “final stage of data interpolation.” Fortunately, being able to do this is a known advantage of HT-SR theory [26, 27]. Second, actual data often follow heavy-tail distributions [28], which can be even more evident in NLP than the more well-behaved datasets in CV [29] that are often used to study generalization.

HT-SR theory. The core principle of HT-SR theory [3, 4, 8, 25] is that HT structures can arise naturally in the ESDs of the weight matrices as the result of extracting various correlations in data during optimization. The main technique used in these papers is to estimate the PL coefficient from the ESDs (which only requires access to weights), with smaller coefficients reported to correspond to higher model quality. However, these estimators can be sensitive to the empirical noise, and so one must be careful not to rely on them alone. For example, the quality of PL fit and the so-called *localization of eigenvectors* [25] should all point to similar conclusions, which could be a sanity check. Fortunately, for large Transformer models [30, 31] typically used in modern NLP tasks, there are many large linear layers, which allows for greater accuracy in the PL

¹As the report of the NeurIPS 2020 Competition on Predicting Generalization in Deep Learning [18] points out, the generalization metric should be able to order models’ performance in a way similar to the generalization gap, and thus it can be used for model selections or neural architecture search; however, see [4] for a detailed exposition of issues with this.

estimators.

The principles of HT-SR theory extend beyond fitting the PL coefficient, however, as ESDs can take many forms. To this end, we study three different types of distributions to fit to the ESDs of weight matrices, including powerlaw (PL) in Eqn. (1), exponentially truncated powerlaw (E-TPL) in Eqn. (2), and exponential (EXP) in Eqn. (3). These are all commonly considered families of distributions in classical studies of PL [32], and it is often hard in practice to predict which family fits data the best (as we show in this paper, this is true for deep NNs especially). Figure 1 shows examples of comparing different HT fittings on the same ESD.

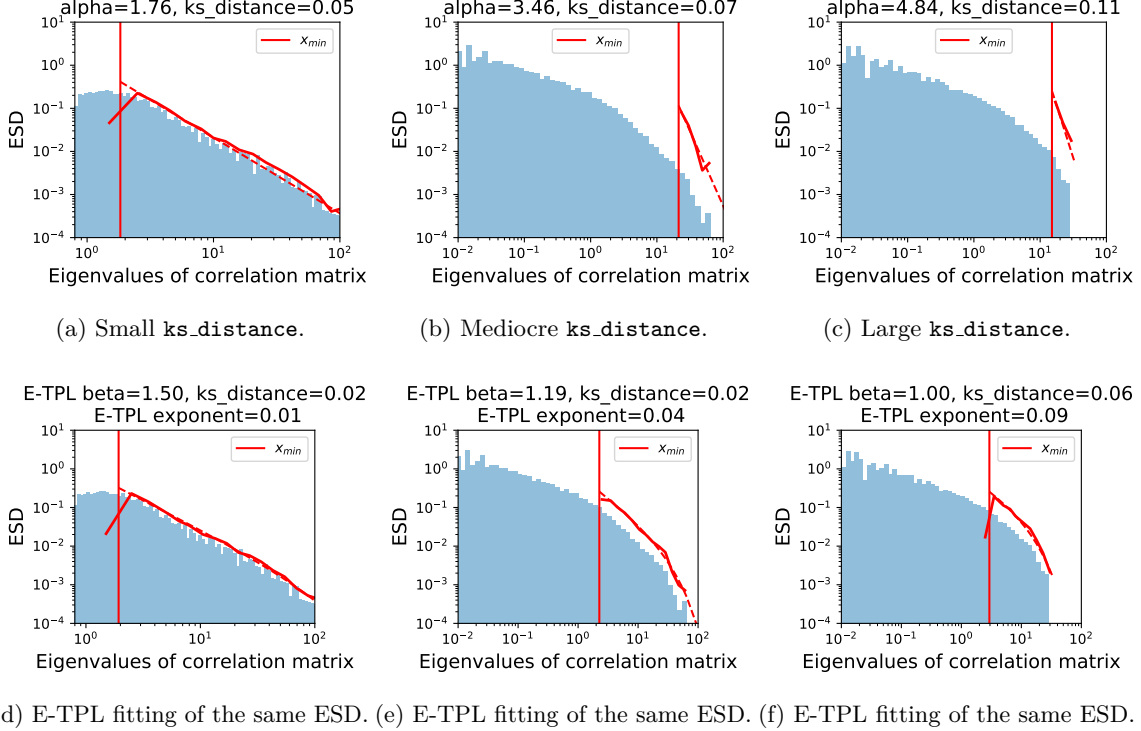


Figure 1: Comparing PL and E-TPL fitting. (First row). Good, mediocre, and bad PL fittings measured by the `ks_distance`. (Second row). E-TPL fitting of the ESD on the same column. Blue histograms represent the ESDs. Solid vertical lines represent the lower threshold x_{\min} found by the fitting procedure. Solid curves represent ESDs truncated using x_{\min} , and dashed curves represent the fitted HT distributions.

When used appropriately, we will find that the various metrics derived from HT-SR, which (following [4]) we call *shape metrics*, uniformly perform better than scale metrics (or norm-based metrics) in our empirical results. Furthermore, while the calculation of more subtle metrics (e.g. those derived from PAC-Bayes bounds) is slow when the data is large, metrics in HT-SR theory are derived from weights and are often much faster to compute.

The following summarizes our main contributions.

- Unlike prior papers on generalization metrics that focus on CV [1, 2], we provide the first systematic empirical study on various generalization metrics in NLP. Compared to existing studies that focus primarily on limited-sized models and data, we consider more practical settings, with Transformers and medium-to-large scale data (e.g., million-scale dataset such as WMT14).
- HT structure is identified as one of the most effective generalization theories in NLP. From our empirical results, shape metrics obtained from the HT ESDs of weight matrices perform uniformly better than norm-based/scale-based metrics for predicting model quality.
- We extend prior studies on HT-SR theory and investigate alternative models to fit heavy-tail/light-tail

distributions. Our results show that the **rand.distance** metric, a novel metric quantifying the distance of the ESD (in distribution) from the randomized layer, and the **exponent** of E-TPL fittings can be used as relatively robust generalization metrics.

2 Background

2.1 Notation and preliminaries

General notation. Consider a NN with d weight matrices $\mathbf{W}_1, \mathbf{W}_2, \dots, \mathbf{W}_d$. We use \mathbf{W} to denote the collection of all the weights and denote the vector that consists of all the model weights as $\text{vect}(\mathbf{W})$. We denote the neural network (function) as $f_{\mathbf{W}}$, which takes a single input sample \mathbf{x} and outputs a vector $f_{\mathbf{W}}(\mathbf{x})$. The superscript init on a weight matrix, e.g. $\mathbf{W}_1^{\text{init}}$, denotes the initial weights from which the model is trained. We use \mathbf{X}_i to denote the correlation matrix, i.e., $\mathbf{X}_i = \mathbf{W}_i^{\top} \mathbf{W}_i$. The notation $\mathbf{1}$ means an all-one vector, and \mathbf{I} means the identity matrix.

Norms and distances. We use different types of norms defined on vectors and matrices. $\|\cdot\|_2$ and $\|\cdot\|_1$ used on vectors respectively means the ℓ_1 norm and the ℓ_2 norm. $\|\cdot\|_F$ and $\|\cdot\|_{\infty}$ used on matrices respectively denotes the Frobenius norm and the spectral norm.

2.2 Preliminary of ESDs of weight matrices

For a weight matrix \mathbf{W}_i , without loss of generality, we denote its shape by $N \times M, N \geq M$. We denote the set of singular values as $\{\sigma_j\}_{j=1}^M$. Following [33], we define the correlation matrix as $\mathbf{X}_i = \mathbf{W}_i^{\top} \mathbf{W}_i$. We denote the eigenvalues of the correlation matrix \mathbf{X}_i as $\{\lambda_j\}_{j=1}^M$, and we have that $\lambda_j = \sigma_j^2$. Furthermore, we use $\lambda_{i,\max}$ to denote the maximum eigenvalue of the correlation matrix \mathbf{X}_i . By ESD of the weight matrix \mathbf{W}_i , we mean the empirical density of the eigenvalues of \mathbf{X}_i , which is usually plotted as a histogram. Following [4], we let $p(x)$ denote the density function to fit the ESD taking values in the interval (x_{\min}, x_{\max}) . For a power law, p satisfies

$$p(x) \propto x^{-\alpha}, \quad x_{\min} < x < x_{\max}. \quad (1)$$

We note that, from [4], x_{\max} is chosen to be the maximum eigenvalue of the correlation matrix. However, x_{\min} is a variable to be optimized to improve the quality of PL fitting, and it is not equal to the minimum eigenvalue in general. We use α_i to denote the fitted PL coefficient of the ESD of the i -th weight matrix \mathbf{W}_i .

Eigenvector localization. The eigenvectors of a random matrix can be localized under certain assumptions on the distributions from which the matrix entries are drawn. Our analysis also considers the localization of an eigenvector $\mathbf{v} = (v_1, v_2, \dots)$, measured by the vector entropy [25]. The vector entropy is calculated using the histogram estimated from the vector entries. Specifically, for an eigenvector \mathbf{v} , a histogram is estimated using a given number of bins b . Then, the histogram is normalized to form a probability vector $\mathbf{P} = (P_1, P_2, \dots, P_b)$. The vector entropy is then calculated as $S(\mathbf{v}) = -\sum_{k=1}^b P_k \log P_k$.

3 Heavy-tail self-regularization theory

In this section, we provide a brief overview of the HT-SR theory, and we discuss several metrics that we derive from it. In HT-SR theory, the ESDs of the weight matrices become more heavy-tailed during training as they become increasingly correlated. One could evaluate the amount of correlations by fitting a PL to the ESD of a weight matrix, using the open-source **WeightWatcher** tool² [3]. After computing the ESD of a weight matrix, we use the maximum likelihood estimate from [34] to fit the PL distribution, the specific form of which has been defined in (1). We use **alpha** to denote the PL coefficient averaged over layers, which is effectively the slope of the tail of the ESD, on a log-log scale.

Correctly identifying and fitting PL distributions is well-known to be a challenge in practice. For example, a density that appears as a straight line on a log-log scale plot need not follow a power law, as there are many

²<https://github.com/CalculatedContent/WeightWatcher>

other distributions that could show a similar behavior, including lognormal and exponential-type distributions [32]. Nested distributions such as E-TPL, which combine the pure PL and other distributional assumptions, can often improve the quality of fitting [32, 34]. Therefore, in addition to the PL distribution defined in (1), we consider several other classes of distributions studied in the literature. Specifically, see the following two additional distributional assumptions.

- (E-TPL exponent) The ESDs are assumed to take the following “nested” form.

$$p(x) \propto x^{-\beta} \exp(-\lambda x), \quad x_{\min} < x < x_{\max}. \quad (2)$$

After fitting the E-TPL, we call the exponential truncation coefficient λ the **exponent** metric.

- (**exp_dist_exponent**). The ESDs are assumed to take the following form.

$$p(x) \propto \exp(-\lambda x), \quad x_{\min} < x < x_{\max}. \quad (3)$$

After fitting the EXP, we call the exponential coefficient λ the **exp_dist_exponent** metric.

Another metric that we introduce is **rand_distance**, which is also a shape metric motivated by the ESDs. We use \mathbf{p}_i to denote the distribution obtained by normalizing the squared singular values of the i -th weight matrix \mathbf{W}_i , and we use $\mathbf{p}_i^{\text{rand}}$ to denote the distribution obtained in the same way but using the randomized weight matrix. Then, we define the **rand_distance** metric as

$$\mu_{\text{rand_distance}} = \frac{1}{d} \sum_{i=1}^d \text{JS}(\mathbf{p}_i, \mathbf{p}_i^{\text{rand}}), \quad (4)$$

where $\text{JS}(\cdot)$ is Jensen-Shannon divergence. This is a distance based on the eigenvalues—not the elements—of a weight matrix and a random initialization matrix. The implementation of **rand_distance** metric can be found in **WeightWatcher**.

For more details of the various metrics considered in this paper, see Table 1. We note that all of the metrics derived from HT-SR do not require the access to data or GPUs. We mainly compare between shape metrics, which are derived from HT-SR, and scale metrics, which are mostly norm-based metrics. For the precise definitions of these metrics, see Appendix A.

Issues of PL fitting. It is well-documented that subtle issues can arise when fitting the ESDs [4, 32–34]. To best mitigate these issues in PL fits and focus on the core mathematical concepts of predicting generalization, we rely on the same strategies used in **WeightWatcher** to fit the ESDs. For example, one issue of PL fitting is correctly choosing the lower threshold x_{\min} . The most common way of doing this [32, 33] is to choose x_{\min} that yields the best quality fit under the Kolmogorov–Smirnov statistic (referred to as **ks_distance** in the sequel; see Eqn. (19).) However, this method is time-consuming, especially for E-TPL as there are two parameters to fit. Therefore, we adopt the “fix-finger” method documented in **WeightWatcher** to select x_{\min} as the peak of the ESD. Besides the speed improvement, we also find this method provides more stable results.

Comparing PL and E-TPL fitting. Referring to Figure 1, we now discuss how E-TPL could partially address these fitting issues. On the first row of Figure 1, we show three typical cases of PL fitting. In Figure 1a, the log-log scale reveals a “linear region” of the histogram, which the PL fitting correctly locates. The quality of fit, measured by the **ks_distance**, is within a typical range, as reported in Table 5 of [25]. In Figure 1b and Figure 1c, the ESDs do not exhibit a clear linear region on the log-log scale. Following [25], it is ill-advised to consider metrics derived from a PL fit in these scenario. In practice, this typically occurs when $\alpha > 4$ (e.g., see Figure 1c). On the other hand, in these two cases, the corresponding E-TPL fits (shown on the second row in Figure 1) still closely match the empirical density function (see Figure 1e and Figure 1f), and the **ks_distance** on the second row using a E-TPL fit is smaller than that for the PL fit on the first row, even when the fit on the second row clearly covers a larger part of the ESD.³ In these two cases,

³We note that the value of **ks_distance** can be effectively made smaller if one restricts to a smaller part of the distribution, as is often done in practice by optimizing the x_{\min} in the (truncated) PL distribution (1). This potential bias is alleviated by using the fix-finger method.

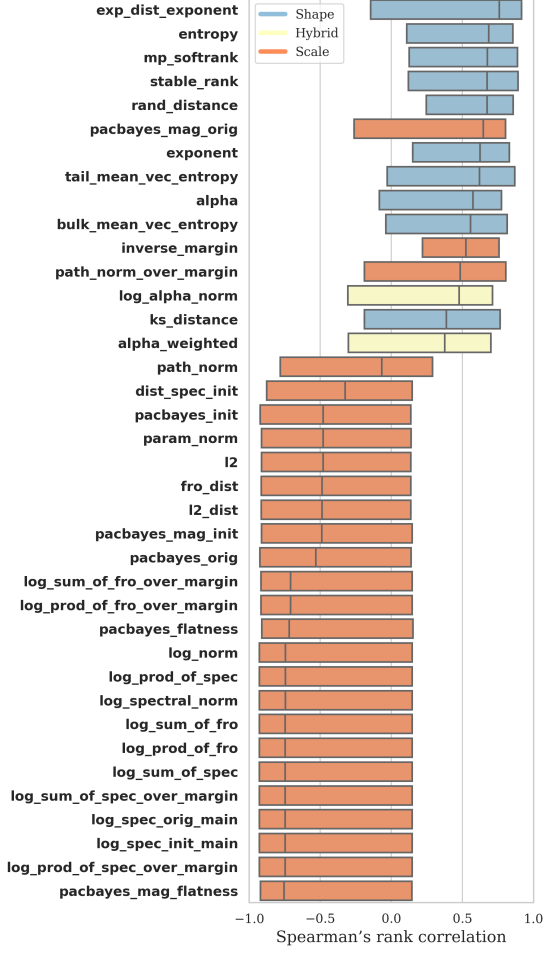
Name	Eqn	Ref	Need initial weights?	Scale or shape	Need data?	Need gpu?	Predicting model quality or generalization gap?
12	(5)	-	No	Scale	No	No	Generalization gap
12.dist	(6)	-	Yes	Scale	No	No	Generalization gap
param.norm	(7)	[1]	No	Scale	No	No	Generalization gap
fro.dist	(8)	[1]	Yes	Scale	No	No	Generalization gap
log.norm	(9)	[25]	No	Scale	No	No	Generalization gap
log.sum.of.fro	(10)	[1]	No	Scale	No	No	Generalization gap
log.spectral.norm	(11)	[4]	No	Scale	No	No	Generalization gap
dist.spec.int	(12)	[1]	Yes	Scale	No	No	Generalization gap
log.prod.of.fro	(13)	[1]	No	Scale	No	No	Generalization gap
log.sum.of.spec	(14)	[1]	No	Scale	No	No	Generalization gap
log.prod.of.spec	(15)	[1]	No	Scale	No	No	Generalization gap
path.norm	(16)	[35]	No	Scale	No	No	Generalization gap
mp.softrank	(17)	[25]	No	Scale/Shape	No	No	Model quality
stable.rank	(18)	[25]	No	Scale/Shape	No	No	Model quality
alpha	(1)	[25]	No	Shape	No	No	Model quality
exponent	(2)	This paper WeightWatcher	No	Shape	No	No	Model quality
exp.dist.exponent	(3)	This paper WeightWatcher	No	Shape	No	No	Model quality
ks.distance	(19)	[25]	No	Shape	No	No	Model quality
tail.mean.vec.entropy	(20)	This paper WeightWatcher	No	Shape	No	No	Model quality
bulk.mean.vec.entropy	(21)	This paper WeightWatcher	No	Shape	No	No	Model quality
entropy	(22)	[25]	No	Shape	No	No	Model quality
rand.distance	(4)	This paper WeightWatcher	No	Shape	No	No	Model quality
alpha.weighted	(23)	[25]	No	Hybrid	No	No	Model quality
log.alpha.norm	(24)	[4]	No	Hybrid	No	No	Model quality
inverse.margin	(27)	[1]	No	Scale	Yes	Maybe	Generalization gap
log.prod.of.spec.over.margin	(28)	[21, 22]	No	Scale	Yes	Maybe	Generalization gap
log.sum.of.spec.over.margin	(29)	[21, 22]	No	Scale	Yes	Maybe	Generalization gap
log.prod.of.fro.over.margin	(30)	[21, 22]	No	Scale	Yes	Maybe	Generalization gap
log.sum.of.fro.over.margin	(31)	[21, 22]	No	Scale	Yes	Maybe	Generalization gap
path.norm.over.margin	(32)	[35]	No	Scale	Yes	Maybe	Generalization gap
pacbeyes.init	(35)	[36]	Yes	Scale	Yes	Yes	Generalization gap
pacbeyes.orig	(36)	[36]	No	Scale	Yes	Yes	Generalization gap
pacbeyes.flatness	(37)	[36]	No	Scale	Yes	Yes	Generalization gap
pacbeyes.mag.init	(38)	[1]	Yes	Scale	Yes	Yes	Generalization gap
pacbeyes.mag.orig	(39)	[1]	No	Scale	Yes	Yes	Generalization gap
pacbeyes.mag.flatness	(40)	[1]	No	Scale	Yes	Yes	Generalization gap

Table 1: Overview of the generalization metrics considered. Our paper focuses on the *shape* metrics derived from the ESDs of weight matrices. See Appendix A for the details of these metrics.

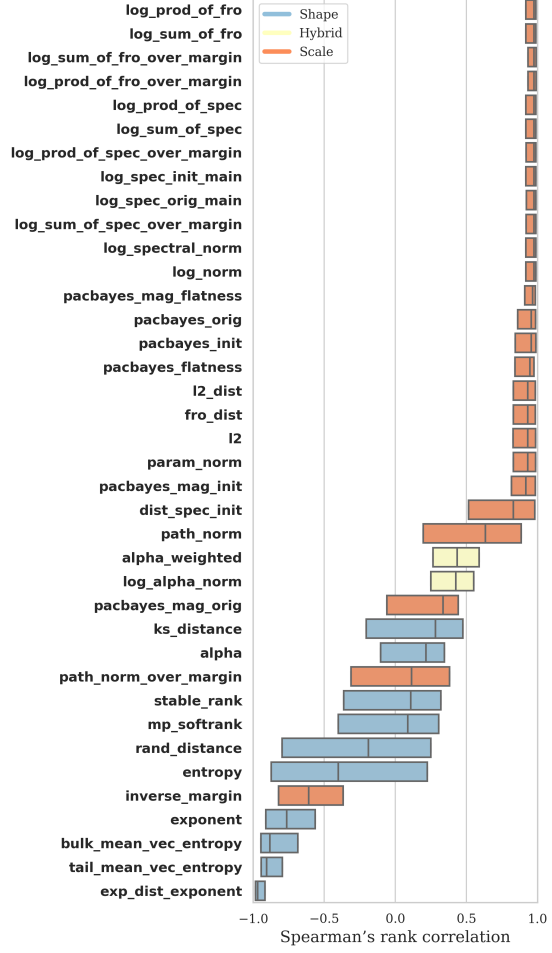
the E-TPL **exponent** plays a similar role as the **alpha** in PL fitting, and provides an effective alternative when the ESD does not exhibit a proper PL.

Between these three PL and E-TPL fittings, we would like to point out that the important thing in HT-SR is not the PL fitting *per se* but that the spectral distributions exhibit HT or other non-standard shapes; the particular forms of the distributions fit here simply constitute different ways to quantify this property in practice. These details, such as selecting the most appropriate distributional assumptions, clearly matter if we would like to engineer the tools of HT analysis to effectively measure the ground truth. However, the primary concern in predicting generalization is to measure the shape information, and the shape information

Correlations with model quality



Correlations with generalization gap



(a) **Correlations with model quality.** Spearman's rank correlation between various generalization metrics and BLEU. (b) **Correlations with generalization gap.** Spearman's rank correlation between various generalization metrics and the generalization gap.

Figure 2: Comparing multiple generalization metrics in terms of predicting the BLEU score (on the left) or the generalization gap (on the right, defined as the training BLEU score subtracted by the test BLEU score). The left, middle and right verticle edge on each box represents the 25/50/75 percentile of the rank correlations in 50 different settings (including different datasets, different amount of data, different network depths, different initial learning rates, and different dropout).

is independent of the fitting procedure, although better fitting procedures may capture the shape information better.

4 Empirical results

In this section, we first give full details of the experimental setup. Then, we provide the analyses of the empirical results.

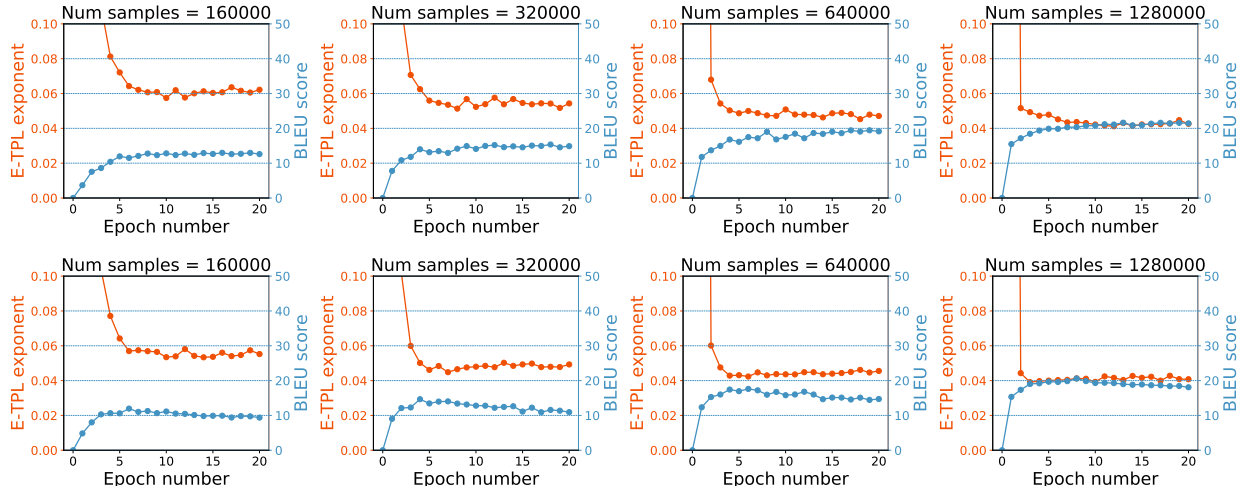


Figure 3: E-TPL exponent closely tracks the BLEU score, i.e., BLEU score increases when the E-TPL exponent drops. Results are shown for Transformers trained on WMT14 with different number of samples. **(First row)**. Training with dropout 0.1. **(Second row)**. Training without dropout.

4.1 Experimental setup

We consider two machine translation datasets, WMT14 [37] and IWSLT [38], which are commonly used as benchmarks for neural machine translation [30, 39–41]. For both datasets, we use German to English (DE-EN). IWSLT consists of 160K parallel bilingual sentence pairs for training, and it is a relatively small-scale dataset. WMT14, on the other hand, has a medium-to-large scale, and it consists of 4.5 million sentence pairs for training. To describe a more holistic picture on the relationship between the generalization metrics and dataset size, and to address the practical concern of training with different amount of data from custom datasets, we subsample the two datasets with different number of samples. Specifically, for IWSLT, we study five cases with {10K, 20K, 40K, 80K, 160K} samples. For WMT14, we study four cases with {160K, 320K, 640K, 1.28M} samples. We intentionally overlap the right end-point (160K) of IWSLT with the left end-point (160K) of WMT14 to study the difference between the two datasets. Similarly, we also study five different values of network depth, including {2, 3, 4, 5, 6}-layer Transformers, and five different levels of initial learning rate. For each combination of (dataset, samples, depth, learning rate), we train both with and without dropout, and we use dropout probability 0.1 when training with dropout. We include the case of training without dropout because we want to study the performance of generalization metrics when there is some extent of overfitting. In total, there are 50 of these training settings. See Appendix B for the details in these 50 settings. We train with three random seeds for each setting.

We follow exactly the training setup in [30], and we develop our implementation based on an online repository⁴ which reproduces the results from [30] with more easily configurable Transformer architectures. We use Transformer-base with 8 attention heads, and an embedding dimension of 512 for both datasets. As we have mentioned earlier, the number of layers ranges from 2 to 6. We train with the inverse square-root learning rate and 10% label smoothing. For each experiment, we train the model for 20 epochs. When calculating the ESDs of the weight matrices, we treat the query, key and value matrices as separate weight matrices.

4.2 Performance of generalization metrics

In this subsection, we study 36 generalization metrics (with details provided in Table 1), and we study how well they are correlated with the BLEU score [24]. We use BLEU score because it is the most commonly

⁴<https://github.com/gordicaleksa/pytorch-original-transformer>

used metric to evaluate machine translation. Also, we are mostly interested in measuring the correlation between the generalization metrics and the test-time BLEU score directly, and we are less interested in the correlation between the generalization metrics to the generalization gap, which is defined as the BLEU score for training subtracted by the BLEU score for test. Nonetheless, we provide the correlation measurement for both the test-time BLEU score and the generalization gap.

4.2.1 E-TPL exponent tracks the BLEU score

As a warm-up, we use our metric `exponent` defined in (2) to track the BLEU score, recalling that `exponent` is derived under the assumption that ESDs follow E-TPLs. We use dropout to study the effect of training schemes, and consider different quantities of data to test robustness in the dataset. Referring to Figure 3, the first row considers models trained with dropout, while the second row considers models trained without dropout. The multiple columns track `exponent` and the BLEU score throughout training for different amounts of data. From the results in Figure 3, we can see that `exponent` not only tracks the BLEU scores but also differentiates underfitting (first row, with dropout) from overfitting (second row, without dropout) in this experiment.

4.2.2 Rank correlation

To systematically evaluate the various metrics considered in this paper, we study the rank correlation between these metrics and the BLEU score. For each of the 50 settings of the hyperparameters and each random seed, we calculate the Spearman’s rank correlation between BLEU scores and the values of each generalization metric over all epochs. The summarized results are presented in Figure 2a. A positive Spearman’s rank correlation (with BLEU) in the plot means that the generalization metric is useful in tracking BLEU during training. A negative Spearman’s rank correlation, on the other hand, means that the metric often gives the wrong prediction. In Figure 2a, we use the average rank correlations for all settings to study the effectiveness of each metric, and present 25% quantile rank correlations to indicate robustness across runs.

From Figure 2a, we see that shape metrics, such as `exp_dist_exponent`, `entropy`, `mp_softrank`, `stable_rank`, `rand_distance`, `exponent`, `alpha`, `ks_distance`, are all among the effective generalization metrics that have a high rank correlation with the BLEU score that measures the model quality of machine translation. In particular, we see that the `rand_distance` metric achieves the highest 25 percent smallest rank correlation. The `exponent` metric, which assumes a E-TPL distribution on the ESDs, achieves the second highest 25 percent smallest rank correlation (we will discuss the problem of the `inverse_margin` metric in Appendix C). The `exp_dist_exponent` metric, which corresponds to the EXP fitting, gives the best average rank correlations. On the other hand, norm-based metrics, such as `log_spectral_norm`, prove ineffective for measuring model quality.

Details of the rank correlation calculations. When calculating the rank correlation, for each generalization metric, we need to associate a positive/negative sign to indicate whether the metric should be positively or negatively correlated with generalization. For example, for the powerlaw coefficient `alpha`, it has been shown in [3, 8, 25, 42] that a smaller `alpha` indicates better model quality. Thus, we associate a negative sign to this metric. However, the metric `rand_distance` implies better model quality when it is larger [25], and so we associate a positive sign to this metric.

4.3 Analysis on the data-dependent metrics

Through the empirical analysis on various metrics, we have obtained some observations that could partially explain why existing data-dependent generalization metrics do not perform well on the NLP tasks.

- **Scale metrics correctly predict the generalization gap instead of the model quality.** We also provide results on the rank correlation between the various generalization metrics and the generalization gap, defined as the training BLEU score subtracted by the test BLEU score. See the results in Figure 2b. It is encouraging to see that most existing generalization metrics give the correct predictions. However,

as we have discussed, we are less interested in this task because correctly predicting the trends of generalization gap does not automatically give predictions on the best-performing models.

- **The PL metrics do not predict the generalization gap.** Since the PL metrics measure self-regularization [8], it is natural to consider whether, like the data-dependent generalization metrics, PL metrics also correlate with the generalization gap. This can easily be seen to be false from Figure 2b.

We expect these observations to be relevant and useful to improve the existing generalization metrics, especially for the NLP tasks that have not been thoroughly investigated before.

Acknowledgements. We would like to acknowledge the IARPA (contract W911NF20C0035), NSF, and ONR for providing partial support of this work. Kannan Ramchandran would like to acknowledge support from NSF CIF-2007669, CIF-1703678, and CIF-2002821. Joseph E. Gonzalez would like to acknowledge supports from NSF CISE Expeditions Award CCF-1730628 and gifts from Alibaba Group, Amazon Web Services, Ant Group, Ericsson, Facebook, Futurewei, Google, Intel, Microsoft, Nvidia, Scotiabank, Splunk and VMware. Our conclusions do not necessarily reflect the position or the policy of our sponsors, and no official endorsement should be inferred.

References

- [1] Yiding Jiang, Behnam Neyshabur, Hossein Mobahi, Dilip Krishnan, and Samy Bengio. Fantastic generalization measures and where to find them. In *International Conference on Learning Representations*, 2019.
- [2] Gintare Karolina Dziugaite, Alexandre Drouin, Brady Neal, Nitarshan Rajkumar, Ethan Caballero, Linbo Wang, Ioannis Mitliagkas, and Daniel M Roy. In search of robust measures of generalization. *Advances in Neural Information Processing Systems*, 33, 2020.
- [3] Charles H Martin, Tongsu Serena Peng, and Michael W Mahoney. Predicting trends in the quality of state-of-the-art neural networks without access to training or testing data. *Nature Communications*, 12(1):1–13, 2021.
- [4] Charles H Martin and Michael W Mahoney. Post-mortem on a deep learning contest: a Simpson’s paradox and the complementary roles of scale metrics versus shape metrics. Technical Report Preprint: arXiv:2106.00734, 2021.
- [5] Preetum Nakkiran, Gal Kaplun, Yamini Bansal, Tristan Yang, Boaz Barak, and Ilya Sutskever. Deep double descent: Where bigger models and more data hurt. In *International Conference on Learning Representations*, 2019.
- [6] Chiyuan Zhang, Samy Bengio, Moritz Hardt, Benjamin Recht, and Oriol Vinyals. Understanding deep learning (still) requires rethinking generalization. *Communications of the ACM*, 64(3):107–115, 2021.
- [7] Jonathan Frankle and Michael Carbin. The lottery ticket hypothesis: Finding sparse, trainable neural networks. In *International Conference on Learning Representations*, 2018.
- [8] Charles H Martin and Michael W Mahoney. Traditional and heavy tailed self regularization in neural network models. In *International Conference on Machine Learning*, pages 4284–4293, 2019.
- [9] Pierre Foret, Ariel Kleiner, Hossein Mobahi, and Behnam Neyshabur. Sharpness-aware minimization for efficiently improving generalization. In *International Conference on Learning Representations*, 2020.

- [10] P Izmailov, AG Wilson, D Podoprikin, D Vetrov, and T Garipov. Averaging weights leads to wider optima and better generalization. In *Conference on Uncertainty in Artificial Intelligence*, pages 876–885, 2018.
- [11] Wuyang Chen, Xinyu Gong, and Zhangyang Wang. Neural architecture search on imagenet in four gpu hours: A theoretically inspired perspective. In *International Conference on Learning Representations*, 2020.
- [12] Zhen Dong, Zhewei Yao, Amir Gholami, Michael W Mahoney, and Kurt Keutzer. HAWQ: Hessian aware quantization of neural networks with mixed-precision. In *IEEE/CVF International Conference on Computer Vision*, pages 293–302, 2019.
- [13] Yaoqing Yang, Rajiv Khanna, Yaodong Yu, Amir Gholami, Kurt Keutzer, Joseph E Gonzalez, Kannan Ramchandran, and Michael W Mahoney. Boundary thickness and robustness in learning models. *Advances in Neural Information Processing Systems*, 33, 2020.
- [14] Thomas Tanay and Lewis Griffin. A boundary tilting persepective on the phenomenon of adversarial examples. *arXiv preprint arXiv:1608.07690*, 2016.
- [15] Timur Garipov, Pavel Izmailov, Dmitrii Podoprikin, Dmitry Vetrov, and Andrew Gordon Wilson. Loss surfaces, mode connectivity, and fast ensembling of dnns. In *Conference on Neural Information Processing Systems*, pages 8803–8812, 2018.
- [16] Stanislav Fort, Huiyi Hu, and Balaji Lakshminarayanan. Deep ensembles: A loss landscape perspective. *arXiv preprint arXiv:1912.02757*, 2019.
- [17] Yaoqing Yang, Liam Hodgkinson, Ryan Theisen, Joe Zou, Joseph E Gonzalez, Kannan Ramchandran, and Michael W Mahoney. Taxonomizing local versus global structure in neural network loss landscapes. In *Thirty-Fifth Conference on Neural Information Processing Systems*, 2021.
- [18] Yiding Jiang, Pierre Foret, Scott Yak, Daniel M Roy, Hossein Mobahi, Gintare Karolina Dziugaite, Samy Bengio, Suriya Gunasekar, Isabelle Guyon, and Behnam Neyshabur. Neurips 2020 competition: Predicting generalization in deep learning. *arXiv preprint arXiv:2012.07976*, 2020.
- [19] Behnam Neyshabur, Srinadh Bhojanapalli, and Nathan Srebro. A PAC-Bayesian approach to spectrally-normalized margin bounds for neural networks. In *International Conference on Learning Representations*, 2018.
- [20] David A McAllester. PAC-Bayesian model averaging. In *Annual Conference on Computational Learning Theory*, pages 164–170, 1999.
- [21] Peter Bartlett, Dylan Foster, and Matus Telgarsky. Spectrally-normalized margin bounds for neural networks. *Advances in Neural Information Processing Systems*, 30:6241–6250, 2017.
- [22] Konstantinos Pitas, Mike Davies, and Pierre Vandergheynst. Pac-bayesian margin bounds for convolutional neural networks. *arXiv preprint arXiv:1801.00171*, 2017.
- [23] Yiding Jiang, Dilip Krishnan, Hossein Mobahi, and Samy Bengio. Predicting the generalization gap in deep networks with margin distributions. In *International Conference on Learning Representations*, 2018.
- [24] Kishore Papineni, Salim Roukos, Todd Ward, and Wei-Jing Zhu. Bleu: a method for automatic evaluation of machine translation. In *Proceedings of the 40th annual meeting of the Association for Computational Linguistics*, pages 311–318, 2002.
- [25] Charles H Martin and Michael W Mahoney. Implicit self-regularization in deep neural networks: Evidence from random matrix theory and implications for learning. *Journal of Machine Learning Research*, 22 (165):1–73, 2021.

- [26] Liam Hodgkinson and Michael W Mahoney. Multiplicative noise and heavy tails in stochastic optimization. In *International Conference on Machine Learning*, pages 4262–4274. PMLR, 2021.
- [27] Liam Hodgkinson, Umut Şimşekli, Rajiv Khanna, and Michael W Mahoney. Generalization properties of stochastic optimizers via trajectory analysis. *arXiv preprint arXiv:2108.00781*, 2021.
- [28] Vitaly Feldman. Does learning require memorization? a short tale about a long tail. In *Proceedings of the 52nd Annual ACM SIGACT Symposium on Theory of Computing*, pages 954–959, 2020.
- [29] Hang Li. Deep learning for natural language processing: advantages and challenges. *National Science Review*, 2017.
- [30] Ashish Vaswani, Noam Shazeer, Niki Parmar, Jakob Uszkoreit, Llion Jones, Aidan N Gomez, Lukasz Kaiser, and Illia Polosukhin. Attention is all you need. In *Advances in neural information processing systems*, pages 5998–6008, 2017.
- [31] Jacob Devlin Ming-Wei Chang Kenton and Lee Kristina Toutanova. Bert: Pre-training of deep bidirectional transformers for language understanding. In *Proceedings of NAACL-HLT*, pages 4171–4186, 2019.
- [32] Aaron Clauset, Cosma Rohilla Shalizi, and Mark EJ Newman. Power-law distributions in empirical data. *SIAM review*, 51(4):661–703, 2009.
- [33] Charles H Martin and Michael W Mahoney. Rethinking generalization requires revisiting old ideas: statistical mechanics approaches and complex learning behavior. Technical Report Preprint: arXiv:1710.09553, 2017.
- [34] Jeff Alstott, Ed Bullmore, and Dietmar Plenz. powerlaw: a python package for analysis of heavy-tailed distributions. *PloS one*, 9(1):e85777, 2014.
- [35] Behnam Neyshabur, Ryota Tomioka, and Nathan Srebro. Norm-based capacity control in neural networks. In *Conference on Learning Theory*, pages 1376–1401. PMLR, 2015.
- [36] Behnam Neyshabur, Srinadh Bhojanapalli, David Mcallester, and Nati Srebro. Exploring generalization in deep learning. *Advances in Neural Information Processing Systems*, 30:5947–5956, 2017.
- [37] Ondřej Bojar, Christian Buck, Christian Federmann, Barry Haddow, Philipp Koehn, Johannes Leveling, Christof Monz, Pavel Pecina, Matt Post, Herve Saint-Amand, et al. Findings of the 2014 workshop on statistical machine translation. In *Proceedings of the ninth workshop on statistical machine translation*, pages 12–58, 2014.
- [38] Mauro Cettolo, Jan Niehues, Sebastian Stüker, Luisa Bentivogli, and Marcello Federico. Report on the 11th iwslt evaluation campaign, iwslt 2014. In *Proceedings of the International Workshop on Spoken Language Translation, Hanoi, Vietnam*, volume 57, 2014.
- [39] Myle Ott, Sergey Edunov, David Grangier, and Michael Auli. Scaling neural machine translation. In *Proceedings of the Third Conference on Machine Translation: Research Papers*, pages 1–9, 2018.
- [40] Dinghan Shen, Mingzhi Zheng, Yelong Shen, Yanru Qu, and Weizhu Chen. A simple but tough-to-beat data augmentation approach for natural language understanding and generation. *arXiv preprint arXiv:2009.13818*, 2020.
- [41] Sergey Edunov, Myle Ott, Michael Auli, and David Grangier. Understanding back-translation at scale. In *Proceedings of the 2018 Conference on Empirical Methods in Natural Language Processing*, pages 489–500, 2018.

- [42] Charles H Martin and Michael W Mahoney. Heavy-tailed universality predicts trends in test accuracies for very large pre-trained deep neural networks. In *SIAM International Conference on Data Mining*, pages 505–513. SIAM, 2020.
- [43] Gamaleldin Elsayed, Dilip Krishnan, Hossein Mobahi, Kevin Regan, and Samy Bengio. Large margin deep networks for classification. *Advances in Neural Information Processing Systems*, 31:842–852, 2018.
- [44] Colin Wei and Tengyu Ma. Improved sample complexities for deep neural networks and robust classification via an all-layer margin. In *International Conference on Learning Representations*, 2019.

A Generalization metrics

In this section, we provide the details of the generalization metrics considered in our analysis. We first define the scale metrics. Then, we define the shape metrics obtained from the ESDs of the weight matrices. Although our focus is on data-independent generalization metrics, we also define generalization metrics based on margin [21, 22] and PAC-Bayesian bounds [19, 20].

A.1 Scale metrics

We first define the metrics motivated from matrix norms and the distance to initialization.

Norm-based and distance-based metrics.

In the following, we discuss multiple metrics obtained from the norms of the weights or the distance between the weights and initialization.

A careful reader might notice that the metrics in this subsection are sometimes averaged over the layers and are sometimes summed over the layers. This inconsistency is simply because we follow the exact definitions from several prior papers. It is worth noting that rank correlation for a single training run, which is the major tool used to compare different metrics, is independent of whether the norm is averaged or summed, as long as the network size does not change during one training run. However, to compare networks with different sizes, proper normalization is necessary.

- (12). The ℓ_2 -norm of vectorized model weights.

$$\mu_{12} = \|\text{vect}(\mathbf{W})\|_2. \quad (5)$$

- (12.dist). The ℓ_2 -distance between the vectorized model weights and the vectorized initial weights.

$$\mu_{12.\text{dist}} = \|\text{vect}(\mathbf{W}) - \text{vect}(\mathbf{W}^{\text{init}})\|_2. \quad (6)$$

- (param_norm). The squared Frobenius norm summed over all weight matrices.

$$\mu_{\text{param_norm}} = \sum_{i=1}^d \|\mathbf{W}_i\|_F^2. \quad (7)$$

- (fro_dist). The distance between a weight matrix and its initilized value, calculated using the Frobenius norm and summed over all layers.

$$\mu_{\text{fro_dist}} = \sum_{i=1}^d \|\mathbf{W}_i - \mathbf{W}_i^{\text{init}}\|_F^2. \quad (8)$$

- (log_norm).

$$\mu_{\text{log_norm}} = \frac{1}{d} \sum_{i=1}^d \log \|\mathbf{W}_i\|_F^2. \quad (9)$$

- (log_sum_of_fro).

$$\mu_{\text{log_sum_of_fro}} = \log d \left(\prod_{i=1}^d \|\mathbf{W}_i\|_F^2 \right)^{1/d}. \quad (10)$$

- (log_spectral_norm).

$$\mu_{\text{log_spectral_norm}} = \frac{1}{d} \sum_{i=1}^d \log \|\mathbf{W}_i\|_\infty^2. \quad (11)$$

- (dist_spec_int).

$$\mu_{\text{dist_spec_int}} = \sum_{i=1}^d \|\mathbf{W}_i - \mathbf{W}_i^{\text{init}}\|_\infty^2. \quad (12)$$

- (`log_prod_of_fro`).

$$\mu_{\text{log_prod_of_fro}} = \log \prod_{i=1}^d \|\mathbf{W}_i\|_F^2. \quad (13)$$

- (`log_sum_of_spec`).

$$\mu_{\text{log_sum_of_spec}} = \log d \left(\prod_{i=1}^d \|\mathbf{W}_i\|_\infty^2 \right)^{1/d}. \quad (14)$$

- (`log_prod_of_spec`).

$$\mu_{\text{log_prod_of_spec}} = \log \prod_{i=1}^d \|\mathbf{W}_i\|_\infty^2. \quad (15)$$

- (`path_norm`). The metric is introduced in [35]. To calculate the metric, we square the parameters of the network, do a forward pass on an all-ones input and then take sum of the network outputs.

$$\mu_{\text{path_norm}} = \|f\mathbf{W}^2(\mathbf{1})\|_1. \quad (16)$$

Scale metrics that require more shape information from the ESDs. The following metrics require more than just the scale information. They either come from specific forms of combined norms that roughly describe the shape of the ESDs, or come from the Marchenko–Pastur (MP) fitting of the ESDs, which makes them different from pure norm-based metrics.

- (`mp_softrank`). The metric is introduced in [25]. To calculate this metric, we fit the MP distribution on the ESD, obtain the bulk max of the MP distribution and then divide by the maximum eigenvalue.

$$\mu_{\text{mp_softrank}} = \frac{1}{d} \sum_{i=1}^d \lambda_{i,\text{MP}} / \lambda_{i,\text{max}}. \quad (17)$$

- (`stable_rank`). The metric is a norm-adjusted measure of the scale of the ESD.

$$\mu_{\text{stable_rank}} = \frac{1}{d} \sum_{i=1}^d \|\mathbf{W}_i\|_F^2 / \|\mathbf{W}_i\|_\infty^2 \quad (18)$$

A.2 Shape metrics

Tail-exponent fitting. The following metrics are derived from fitting the ESDs using a heavy or light-tail distribution.

- (`alpha`). The slope of the tail of the ESD, on a log-log scale. We use MLE from [34] to estimate `alpha`. The distribution of eigenvalues is assumed to have the form of (1).
- (`exponent`). The tail exponent of the E-TPL fitting of the ESD. This is a new generalization metric introduced in this paper.
- (`exp_dist_exponent`). The tail exponent of the EXP fitting of the ESD, under the assumption that the ESD follows an exponential distribution (3). This is a new generalization metric introduced in this paper.
- (`ks_distance`). The Kolmogorov-Smirnoff (KS) goodness-of-fit test of the powerlaw fitting.

$$\mu_{\text{ks_distance}} = \frac{1}{d} \sum_{i=1}^d \sup_x |F_i^*(x) - S_i(x)|, \quad (19)$$

where $F_i^*(x)$ is the fitted powerlaw distribution on the ESD, and $S_i(x)$ is the ESD itself.

Vector localization. The following metrics are derived from the localization of eigenvectors. In this part, we use $\lambda_{i,j}$ and $\mathbf{v}_{i,j}$ to denote the j -th eigenvalue and eigenvector of the i -th correlation matrix \mathbf{X}_i .

- (**tail_mean_vec_entropy**). The mean of the vector entropies of the eigenvectors corresponding to eigenvalues on the tail of the ESD.

$$\mu_{\text{tail_mean_vec_entropy}} = \frac{1}{d} \sum_{i=1}^d \text{MEAN}(\{S(\mathbf{v}_{i,j}) | \lambda_{i,j} > \lambda_{i,\min}\}). \quad (20)$$

- (**bulk_mean_vec_entropy**). The mean of the vector entropies of the eigenvectors corresponding to eigenvalues on the bulk of the ESD.

$$\mu_{\text{bulk_mean_vec_entropy}} = \frac{1}{d} \sum_{i=1}^d \text{MEAN}(\{S(\mathbf{v}_{i,j}) | \lambda_{i,j} \leq \lambda_{i,\min}\}). \quad (21)$$

Metrics from the eigenvalues. The following two metrics are derived using the eigenvalues of a weight matrix normalized as probabilities. Recall that we use \mathbf{p}_i to denote the distribution obtained by normalizing the squared singular values of \mathbf{W}_i , and we use $\{p_{i,j}\}_{j=1}^b$ to denote the empirical distribution with b bins.

- (**entropy**). The entropy of the squared eigenvalues of a weight matrix, normalized as probabilities. This metric is also known as the Generalized von-Neumann Matrix Entropy.

$$\mu_{\text{entropy}} = \frac{1}{d} \sum_{i=1}^d \frac{-1}{\log(R(\mathbf{W}_i))} \sum_j p_{i,j} \log p_{i,j}, \quad (22)$$

where $R(\cdot)$ is the rank of a matrix.

- (**rand_distance**). The distance in distribution from the randomized layer. See the definition in Eqn. (4).

A.3 Hybrid metrics

The following metrics are scaled versions of **alpha**. They require both the shape information from **alpha** and the scale information from other weight norms.

- (**alpha_weighted**). A scale-adjusted form of **alpha**. This metric is called $\hat{\alpha}$ in [3, 4, 25].

$$\mu_{\text{alpha_weighted}} = \frac{1}{d} \sum_{i=1}^d \alpha_i \log \lambda_{i,\max}. \quad (23)$$

- (**log_alpha_norm**). This metric is another scale-adjusted **alpha** metric in the form of Schatten norm. Recall that we use $\{\lambda_j\}_{j=1}^M$ to denote the set of eigenvalues of the correlation matrix $\mathbf{X}_i = \mathbf{W}_i^\top \mathbf{W}_i$, where \mathbf{W}_i is the N -by- M weight matrix that satisfies $N \geq M$. Then, we can define the Schatten p -norm as the following.

$$\|\mathbf{X}_i\|_p = \left(\sum_{j=1}^M \lambda_j^p \right)^{\frac{1}{p}}. \quad (24)$$

Using this definition, we can define the metric **log_alpha_norm** as the following.

$$\mu_{\text{log_alpha_norm}} = \frac{1}{d} \sum_{i=1}^d \log \|\mathbf{X}_i\|_{\alpha_i}^{\alpha_i}. \quad (25)$$

A.4 Margin-based metrics

Then, we discuss generalization metrics motivated from margins. Recall that we use $f_{\mathbf{W}}$ to denote the neural network with weights \mathbf{W} . For a multi-class classification problem with sample-label pair (\mathbf{x}, y) , we define margin as the following.

$$\gamma(\mathbf{x}, y, f_{\mathbf{W}}) = (f_{\mathbf{W}}(\mathbf{x}))[y] - \max_{i \neq y} f_{\mathbf{W}}(\mathbf{x})_i. \quad (26)$$

For machine translation, we consider the margin of each output token. We note that the number of classes, or the number of possible tokens, is often particularly large for machine translation, which is at least in the order of thousands.

Following [1], we consider output margins only⁵, and we use the 10th percentile of the margin distribution calculated from the entire training set as a robust surrogate for the minimum margin. Using the margin γ defined as the 10th percentile, we define several generalization metrics.

- (inverse_margin).

$$\mu_{\text{inverse_margin}} = \frac{1}{\gamma^2}. \quad (27)$$

- (log_prod_of_spec_over_margin).

$$\mu_{\text{log_prod_of_spec_over_margin}} = \log \frac{\prod_{i=1}^d \|\mathbf{W}_i\|_\infty^2}{\gamma^2} = \mu_{\text{log_prod_of_spec}} - 2 \log \gamma. \quad (28)$$

- (log_sum_of_spec_over_margin).

$$\mu_{\text{log_sum_of_spec_over_margin}} = \log d \left(\frac{\prod_{i=1}^d \|\mathbf{W}_i\|_\infty^2}{\gamma^2} \right)^{1/d} = \log d + \frac{1}{d} (\mu_{\text{log_prod_of_spec}} - 2 \log \gamma). \quad (29)$$

- (log_prod_of_fro_over_margin).

$$\mu_{\text{log_prod_of_fro_over_margin}} = \log \frac{\prod_{i=1}^d \|\mathbf{W}_i\|_F^2}{\gamma^2} = \mu_{\text{log_prod_of_fro}} - 2 \log \gamma. \quad (30)$$

- (log_sum_of_fro_over_margin).

$$\mu_{\text{log_sum_of_fro_over_margin}} = \log d \left(\frac{\prod_{i=1}^d \|\mathbf{W}_i\|_F^2}{\gamma^2} \right)^{1/d} = \log d + \frac{1}{d} (\mu_{\text{log_prod_of_fro}} - 2 \log \gamma). \quad (31)$$

- (path_norm_over_margin).

$$\mu_{\text{path_norm_over_margin}} = \frac{\mu_{\text{path_norm}}}{\gamma^2}. \quad (32)$$

A.5 Metrics derived from PAC-Bayesian bounds

Several well-known generalization bounds are derived using the PAC-Bayesian framework, which bounds the generalization gap using the KL-divergence between a predefined prior distribution (usually chosen as Gaussian) and the posterior distribution of the trained models. The key component of the PAC-Bayesian bounds used in most existing implementations is the procedure of searching for the largest magnitude of Gaussian perturbation, denoted as σ , such that the perturbed weights of the neural network achieve a bounded increase in the training loss. More specifically, σ is defined such that

$$\mathbb{E}_{\mathbf{U} \sim \mathcal{N}(\mathbf{0}, \sigma^2 \mathbf{I})} [\text{TrainLoss}(f_{\mathbf{W}+\mathbf{U}})] \leq \text{TrainLoss}(f_{\mathbf{W}}) + \delta, \quad (33)$$

where δ is a predetermined threshold, and it is chosen as 0.5 in the experiments on machine translation. Similarly, one can define “magnitude-aware” perturbation with magnitude σ' , such that

$$\mathbb{E}_{\mathbf{U}} [\text{TrainLoss}(f_{\mathbf{W}+\mathbf{U}})] \leq \text{TrainLoss}(f_{\mathbf{W}}) + \delta, \quad (34)$$

where each weight entry u_i in \mathbf{U} is distributed as $\mathcal{N}(0, \sigma'^2 |w_i|^2 + \epsilon^2)$, and ϵ is chosen as 1e-3 [2]. Given the perturbation magnitude σ , the magnitude-aware perturbation σ' and the number of samples m , one can define the following generalization metrics.

⁵We note that margins can be defined in any layer [13, 43, 44].

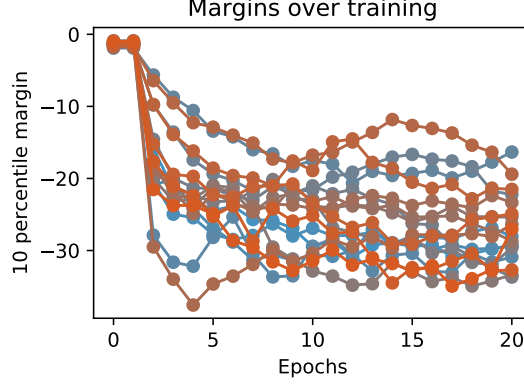


Figure 4: The margins remain negative in the experiments on machine translation due to the large alphabet size.

- (pacbeyes_init).

$$\mu_{\text{pacbeyes_init}} = \frac{\mu_{12.\text{dist}}^2}{4\sigma^2} + \log \frac{m}{\sigma} + 10. \quad (35)$$

- (pacbeyes_orig).

$$\mu_{\text{pacbeyes_orig}} = \frac{\mu_{12}^2}{4\sigma^2} + \log \frac{m}{\sigma} + 10. \quad (36)$$

- (pacbeyes_flatness).

$$\mu_{\text{pacbeyes_flatness}} = \frac{1}{\sigma^2}. \quad (37)$$

- (pacbeyes_mag_init).

$$\mu_{\text{pacbeyes_mag_init}} = \frac{1}{4} \sum_{i=1}^{\omega} \log \left(\frac{\epsilon^2 + (\sigma'^2 + 1)\mu_{12.\text{dist}}^2/\omega}{\epsilon^2 + \sigma'^2|w_i - w_i^{\text{init}}|^2} \right) + \log \frac{m}{\sigma} + 10. \quad (38)$$

- (pacbeyes_mag_orig).

$$\mu_{\text{pacbeyes_mag_orig}} = \frac{1}{4} \sum_{i=1}^{\omega} \log \left(\frac{\epsilon^2 + (\sigma'^2 + 1)\mu_{12}^2/\omega}{\epsilon^2 + \sigma'^2|w_i - w_i^{\text{init}}|^2} \right) + \log \frac{m}{\sigma} + 10. \quad (39)$$

- (pacbeyes_mag_flatness).

$$\mu_{\text{pacbeyes_mag_flatness}} = \frac{1}{\sigma'^2}. \quad (40)$$

B Additional details on the experiment setup

There are 50 different settings that we consider for our experiments. See Table 2. The column titled with “initial learning rate” shows the constant factor multiplied with the standard learning rate schedule. Given the embedding dimension d_e , step number t , number of warm-up steps t_w , the formula for the inverse square-root learning rate schedule is the following.

$$\text{Learning Rate} = d_e^{-0.5} \cdot \min(t^{-0.5}, t \cdot t_w^{-1.5}). \quad (41)$$

C Additional analysis on scale metrics

In this section, we discuss an issue of computing margin-based generalization metrics. Generically, these bounds are of the form

$$L(f) \leq \hat{L}_\gamma(f) + C/\gamma$$

where $L(f)$ is the population error, \hat{L}_γ is the training margin loss at margin γ , typically

$$\sum_{(x,y) \in S} \mathbf{1}\{\max_j f(x)_j \leq \gamma + f(x)_y\},$$

and C is some complexity term. First, note that this construction requires the margin γ to be positive. Moreover, the training margin loss is an increasing function of γ , while the complexity term C/γ is decreasing in γ , thus the conventional way of using the margin bound is to optimize over the margin to balance two terms in the margin bound [21], rather than pre-specifying the value of the margin dependent on the data. However, we choose to follow the related papers [1, 2], and we use the 10th percentile margin as a robust estimate of the minimum margin in the dataset. We use this margin in all of the margin-normalized generalization metrics. However, in all of the experiments on machine translation, the 10th percentile margin remains negative throughout the whole training, violating the requirement that the bound is evaluated at a positive value of margin. See Figure 4. This problem results from the large Alphabet for machine translation, which makes it difficult to fully interpolate the data, and hence makes the margin-normalized generalization metrics in [1, 2] hard to be applicable to the present setting.

Table 2: Parameter settings of empirical studies in Section 4.

Index	Purpose of the experiment	Dataset	Number of samples	Initial learning rate	Network depth	Dropout (Yes/No)	Number of training epochs
0	Different amount of data in IWSLT	IWSLT	10K	1	6	Yes	20
1		IWSLT	10K	1	6	No	20
2		IWSLT	20K	1	6	Yes	20
3		IWSLT	20K	1	6	No	20
4		IWSLT	40K	1	6	Yes	20
5		IWSLT	40K	1	6	No	20
6		IWSLT	80K	1	6	Yes	20
7		IWSLT	80K	1	6	No	20
8		IWSLT	160K	1	6	Yes	20
9		IWSLT	160K	1	6	No	20
10	Different learning rate in IWSLT	IWSLT	160K	0.75	6	Yes	20
11		IWSLT	160K	0.75	6	No	20
12		IWSLT	160K	0.5	6	Yes	20
13		IWSLT	160K	0.5	6	No	20
14		IWSLT	160K	0.375	6	Yes	20
15		IWSLT	160K	0.375	6	No	20
16		IWSLT	160K	0.25	6	Yes	20
17		IWSLT	160K	0.25	6	No	20
18	Different network depth in IWSLT	IWSLT	160K	1	5	Yes	20
19		IWSLT	160K	1	5	No	20
20		IWSLT	160K	1	4	Yes	20
21		IWSLT	160K	1	4	No	20
22		IWSLT	160K	1	3	Yes	20
23		IWSLT	160K	1	3	No	20
24		IWSLT	160K	1	2	Yes	20
25		IWSLT	160K	1	2	No	20
26	Different amount of data in WMT	WMT	160K	1	6	Yes	20
27		WMT	160K	1	6	No	20
28		WMT	320K	1	6	Yes	20
29		WMT	320K	1	6	No	20
30		WMT	640K	1	6	Yes	20
31		WMT	640K	1	6	No	20
32		WMT	1.28M	1	6	Yes	20
33		WMT	1.28M	1	6	No	20
34	Different learning rate in WMT	WMT	1.28M	0.75	6	Yes	20
35		WMT	1.28M	0.75	6	No	20
36		WMT	1.28M	0.5	6	Yes	20
37		WMT	1.28M	0.5	6	No	20
38		WMT	1.28M	0.375	6	Yes	20
39		WMT	1.28M	0.375	6	No	20
40		WMT	1.28M	0.25	6	Yes	20
41		WMT	1.28M	0.25	6	No	20
42	Different network depth in WMT	WMT	1.28M	1	5	Yes	20
43		WMT	1.28M	1	5	No	20
44		WMT	1.28M	1	4	Yes	20
45		WMT	1.28M	1	4	No	20
46		WMT	1.28M	1	3	Yes	20
47		WMT	1.28M	1	3	No	20
48		WMT	1.28M	1	2	Yes	20
49		WMT	1.28M	1	2	No	20